Surface Analysis of Silicon (100) Wafer After Contact Electrification Using Kelvin Force Microscopy

Jose M. Esmeria, Jr.,[1, 2] Romeric Pobre[1]

[1]Physics Department, De La Salle University, 2401 Taft Avenue, Manila 1004, Philippines
[2]Reliability Engineering Department, TDK Philippines Corporation (TPC), 119 East Science Avenue, SEPZ, Biñan, Laguna 4024, Philippines.

*Corresponding Author: jose_esmeria@dlsu.edu.ph

ABSTRACT

Contact electrification was demonstrated on Si (100) wafer, and surface charge images at submicron scale were analysed using Kelvin force microscopy (KFM). Potential map images have shown carpet-like patterns on the (100) plane of Si wafer. Individual potential spikes that appeared on the surface are indicative of the presence of charges arising from contact electrification. It was clearly shown that positive and negative surface potential maps on Si (100) wafer with low resistivity have minimal change in the order of ±2.5 mV after 4800 seconds of noncontact electrification. The mechanism for the slow discharged on the Si (100) wafer can be modelled like a clamped capacitor direct current (D.C.) electric circuit.

Keywords: Surface interfaces, Contact electrification, Triboelectricity.

INTRODUCTION

A significant number of researches have been done for the last 50 years in contact electrification (CE). CE or triboelectricity has beneficial applications in medical sensors , body implants, pharmaceuticals and photocopying (Lacks & Mohan Sankaran, 2011), and microelectric generators (Zhou et al., 2013). However, charges generated through CE are a prelude to a charge device model (CDM) type of electrostatic discharge (ESD) damage to electronic devices. Typical ESD damage associated with CDM is <125 V for class C1 devices ("Part 5: Device Sensitivity and Testing » Electro Over-Stress (EOS) /ESD Association, Inc.," n.d.). Moreover, HDD read/write sensors have even lower threshold at <1 V (Baril, Nichols, & Wallash, 2002). CE is a well-known phenomenon, but the fundamental mechanisms behind CE are not yet fully understood (Lacks & Mohan Sankaran, 2011). Current understanding of CE revolves around the idea that when two materials are brought into surface contact and made to separate, each surface will produce uniform but oppositely electric charge distribution. Depending on the type of material, electric charges may decay rapidly upon contact to ground (or ionization) for dissipative materials or charges may stay longer for insulators. A common way to determine material's charge affinity—either positive or negative—is thru the use of triboelectric series (Diaz & Felix-Navarro, 2004). Triboelectric series is based from empirical method that sequences materials based from their charge transfer from the positive (+top) to the negative (−bottom). When two different materials contact and separates (CE), the material listed at positive (+) side will likely be charged positively and the negative (−) side will be charged negatively. However, the amount of electric charge generated on the surface of two materials after CE is dependent on the applied force, room humidity, and ground continuity of the material (Hogue, 2004).

Triboelectric charging between two different metals is widely accepted as an exchange of electrons due to their work function difference. This difference is brought about by the difference of the individual Fermi levels of both metals where some electrons flow from metal with higher Fermi level into the other metal (Williams, 2012). It was also reported that triboelectric charging for polymers can be best explained by two well-known mechanisms, one involving electron transfer and the other due to the presence of ions on the surface of the material. Electron transfer on an insulator was reported to be a function of its physical condition, and surface impurities, such as ion contaminants, could well influence tribocharging (Diaz & Felix-Navarro, 2004). The use of atomic force microscopy has made advances in the in the study of contact electrification at nanometer levels (Gady, Reifenberger, & Rimai, 1998). By attaching 5-µm spheres on the AFM tip, these spheres act as CE applicators on dielectric substrates. With this early setup, contact electrification was studied using force interactions between the sphere and the sample. Later, potential mapping (Melitz, Shen, Kummel, & Lee, 2011) by Kelvin force microscopy or KFM—a special function of atomic force microscope or AFM—were mostly utilized to characterize surface electric potentials. KFM was also instrumental in demonstrating mosaic patterns of both positive and negative charge for each material after contact for polymer specimens (Baytekin, Patashinski, Branicki, & Baytekin, 2011). Aside from the mosaic charge patterns, of both positive and negative charge distributions, the study also showed material transfer and changes in surface composition occurred after contact electrification. Another study suggested that these mosaic patterns are thought to be an outcome of some complex mechano-chemical reactions (Sakaguchi, Makino, Ohura, & Iwata, 2014). These ions on the surface are formed from molecular bond breaking that arises after triboelectrification where radicals are formed on each opposing surfaces (Mazur & Grzybowski, 2017, p. 2025). Studies on contact electrification using EFM or KFM were mostly related to insulators and prepared polymers, which show potential maps of the surfaces using the tip as a contact electrifying tool. These KFM studies used in situ techniques to measure triboelectrification after frictional-force applications by utilizing an AFM cantilever tip. These techniques were able to perform a comparative analysis of triboelectrification and contact electrification (Zhou, Li, Niu, & Wang, 2016) for a dielectric sample. AFM-KFM was also used to analyze semiconductor materials like SiO_2 under atmospheric conditions (Zhou et al., 2013) as well as n-type GaAs (Brunkov et al., 2013), which had a measured surface potential of 6 mV. Furthermore, similar material (Shiota, n.d.) using Si (111) was performed at ultrahigh vacuum (UHV) AFM by scratching the surface of Si the with an uncoated AFM Si tip as a CE generator, in which a negative charge pattern was observed and measured to be −0.1 V at its peak.

Si is a common semiconductor material and is widely used as a base material for almost all electronic devices. These novel techniques using the tip for contact electrification can quantify both the charge distribution and the force applied (Cai & Yao, 2016); however, a real-world scenario depends on the common material in contact. An industrial-type Q tip or cotton tip, for example, is a common material for touch-up and removal of contamination in electronics manufacturing. These tools are usually used in the final inspection process of manufacturing, prior to shipment. Therefore, it is in the interest of this work to study the effects of contact electrification of a semiconductor surface using a common touch-up tool and propose a model for the charge decay at the surface of Si sample after CE.

KFM

Surface potential microscopy or SPM (Melitz, Shen, Kummel, & Lee, 2011) is a special function of an AFM, and it is also known commonly as KFM, which produces images of potential maps from the scanned surface. The cantilever tip function is related to the energy of the capacitance C between the tip and the sample. The electrostatic force between the tip and sample surface is then related to the rate of changes of energy that

$$F_{ef}(z) = -\frac{1}{2}\frac{dC(z)}{dz}(\Delta V)^2 \quad (1.0)$$

where is the voltage difference between tip and sample. Where is the capacitance gradient with respect to z, which is the vertical distance between sample and tip. Whereas is defined as

$$\Delta V = V_{ac}(t) + V_{dc} + V_{cd} \quad (2.0)$$

where and are the DC bias voltage on the tip, is the AFM oscillating drive voltage on tip and is the resonant frequency of the cantilever, and is contact potential due to work function difference between tip (and sample and is expressed as

$$V_{cd} = \frac{(\emptyset_s - \emptyset_t)}{q} \quad (3.0)$$

q is the electronic charge. Substituting (3.0) to (2.0) and then to (1.0), therefore, the electrostatic force exerted between the tip and sample can be represented as (Melitz et.al., 2011)

$$F_{ef}(z) = -\frac{1}{2}[V_{cd} + V_{dc} + V_{ac}sin\omega t]^2\frac{\partial C(z)}{\partial z} \quad (4.0)$$

Thus, potential map images have two components: tip bias (and) and capacitance gradient . Thus, capacitance gradient is influenced by the surface charge density on the surface of the sample. Therefore, the change in surface charge density changes the force on the tip and therefore changes the potential image of the surface.

AFM commonly uses a tapping mode to scan the surface ("Basic Theory Atomic Force Microscopy (AFM)," n.d.) to obtain its physical topography. In this method, the tip lightly touches the surfaces (thus tapping) at its oscillating frequency (60 to 100 kHz) while maintaining constant oscillation amplitude to generate the image. The tapping mode produces high-resolution imaging without leaving artefact or damage on the surface of the samples. The topographic image generated by tapping mode AFM is often called *height* image.

SPM on the other hand utilizes the same tapping initially to generate *height* images. *Height* images are stored, and the tip then lifts up to a certain height point called *z* height. Utilizing the stored image from the previous tapping mode scan, the entire surface is scanned again at a fixed amplitude set point A_O, which followed the potential gradient of the surface. This second image is then interleaved with the first image to generate surface potential image as shown in Figure 1.

The SPM (KFM) imaging techniques used in this experiment will give some insights into changes of the material surfaces after contact electrification, using a practical common touch in manufacturing such as the cotton Q tip.

MATERIALS AND METHODS

A 5-mm × 5-mm *n*-type Si wafer (100) (SUMCO Corporation) was used as a sample for this experiment. Using conventional AFM function, the silicon wafer flatness was measured to be 0.12 nm ± 0.2 nm for a scan length of 40 μm with an average surface roughness of 0.26 nm. The sample was cleaned using a similar type of cotton Q-tip soaked with 2-propanol; its surface was wiped in one direction and then left to dry at room temperature for 300 seconds. This procedure was to mitigate the effects of contamination during 2D scanning. The sample was attached to a conductive carbon double-sided tape on a 3-mm × 1-mm stainless steel disk.

A cleanroom-grade industrial cotton Q-tip (HUBY340) («3» Cotton Applicator | Clean Cross,» n.d.) was used as surface applicator on the Si wafer to generate contact electrification. Figure 3 shows the type of cotton Q-tip used in these experiments and the SEM image of the cotton fiber at 10,000×, showing a small particle encircled in the picture. The swab was rubbed more than five times, and each rub has an equivalent down force of 100-g weight pressed on the surface of the Si (100) wafer. The Si is scanned initially to image the uncharged surface, then the sample was retracted from the AFM to perform contact electrification. Field of view is set at 1 μm × 1

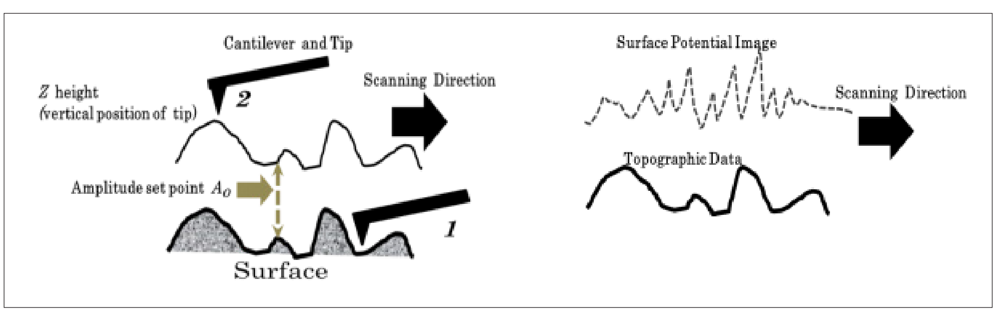

Figure 1. Concept of AFM-KFM.

μm with an image aspect ratio of 1:1. A grooved marker was utilized to scan the exact location of the scanned section of the Si wafer after contact electrification as shown in Figure 2.

A commercially available Bruker Dimension ICON Atomic Force Microscope (AFM) with Surface Potential Microscopy (SPM) modes was utilized for the experiment. The AFM resolution is 0.01 nm, and the tips used were commercially available n-type MESP-RC silicon tips with CoCr coating from Bruker ("AFM Probes | AFM Cantilever | AFM Tips - Bruker AFM Probes," n.d.). It has a nominal radius of about 20 nm, and a tip resonant frequency ranging from 70 kHz to 80 kHz was used for both imagings. The tip was biased by about +1 V in order to set the appropriate dynamic range on the images. Height images were used as reference for both modalities to determine if the changes in the surface structures are created by surface defects or from airborne materials.

All experiments were done in a laboratory at a room temperature of 22±4°C and a relative humidity (RH) of 50±5%.

RESULTS AND DISCUSSION

AFM Topographic and KFM Surface Potential Images

Figures 4A and 4B show the topographic (*height*) images in nanometers using AFM with a scan size of 1 μm × 1 μm, before and after CE, respectively. This height image serves as reference before SPM imaging. It is noted that the surface of Si after does not significantly change, except for some bright protruding dots. This change in surface texture is a result of when cotton and Si surface make contact or are rubbed against each other. The bright dots in Figure 4B are indicative of foreign material left behind during CE.

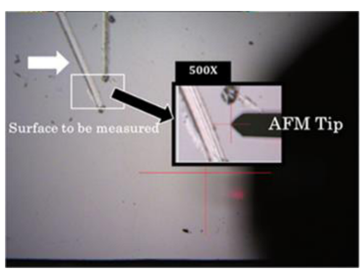

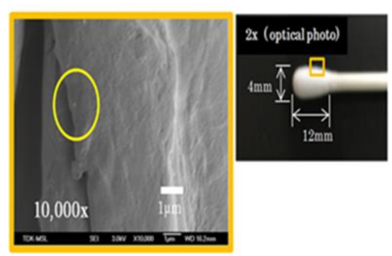

Figure 2. Groove marker on Si (100) wafer surface.

Figure 3. Cotton swab fiber magnified 10,000× using FE-SEM.

a) BEFORE CE Topographic image b) AFTER CE Topographic Image

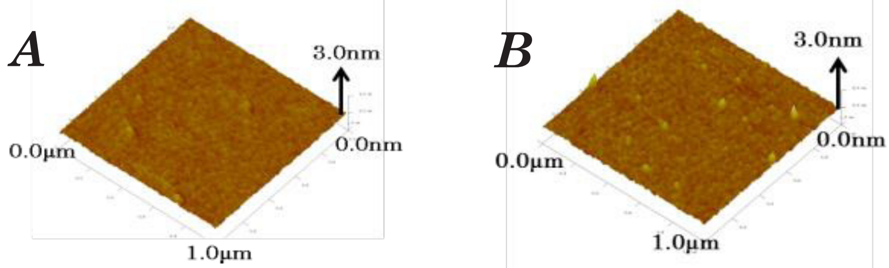

Figure 4. AFM images of n-type Si.

Using SPM imaging the surface before CE is shown in Figure 3C together with the charged surface in Figure 4D after CE. The surface before CE shows a mosaic but smooth pattern, whereas the surface after CE image shows a *carpet-like* surface, wherein individual spikes distance between each other is approximately 17 nm ± 10 nm, based from the image sectional analysis as shown in Figure 6. The mosaic-like pattern is images of charge distribution on the surface before CE; after CE, the carpet-like image in the surface appeared, which is composed of positive (light color) and negative (dark color), as shown in the inset image.

KFM images were also taken using 5-μm × 5-μm scan size using the same type of cotton Q-tip and the same methodology for generating CE. Figures 7A and 7B show the Si (100) wafer that manifested the same *carpet-like* image similar to Figure 5 with peak distances of approximately 13 nm ± 5 nm.

KFM Image Comparison of Cotton, Muscovite Mica, and Silicone Rubber

Cotton is reported to be neutral, or its charge affinity is very small in the triboelectric series (Diaz & Felix-Navarro, 2004). This is the reason why cotton Q-tips are commonly used in the electronic industries as a touch-up tool to minimize damage on electronic devices. To compare the surface potential image of the Si (100) wafer after CE, two insulator-type materials, namely, muscovite mica ($KAl_2(SI_3Al)O_{10}(OH)_2$) and silicone rubber were used to compare with cotton. Silicone rubber, which is based from polydimethylsiloxane (PDMS), has a negative (−) charge affinity, while muscovite mica has a positive (+) charge affinity in the triboelectric series (Lacks & Mohan Sankaran, 2011).

Using a silicone (Fuji Silicone) rubber, CE was performed by rubbing the Si surface five times in one direction, with a downward force approximately at 300 g. Figures 7C and 7D show the similar carpet-like images in the figure 5d Si (100) wafer. Since silicone negative charge affinity is lower than cotton in the triboelectric series, the surface potential image would have a higher positive spike intensity compared to cotton in Figure 7b. Each peak distance was approximately 12 ± 5 nm. The muscovite mica used for applying CE was a (Muscovite Mica Substrates: SPI Supplies, n.d.) disk with a 12-mm diameter and 0.15-mm thickness. This disk was placed on top of the Si samples and pressed using a 200-g stainless steel weight for about 600 seconds.

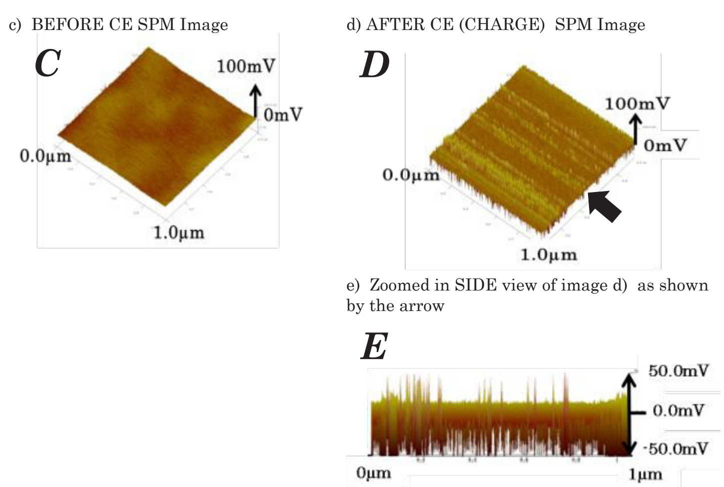

Figure 5. Si KFM images of the Si (100) wafer and side view of the carpet-like images showing positive and negative spikes.

a) TOP VIEW 2D image of the surface potential map

b) Plot of the line section (yellow line).

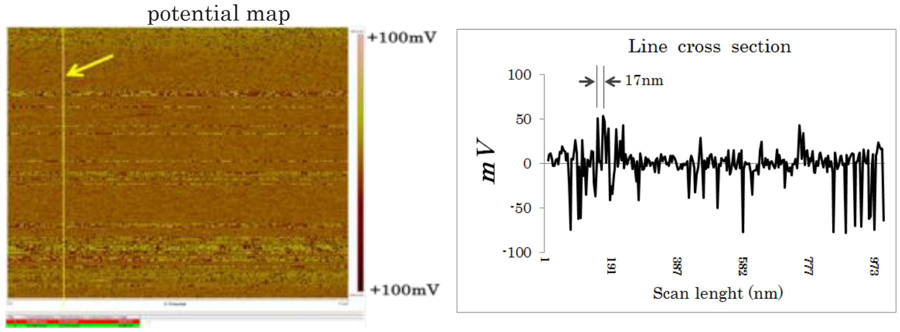

Figure 6. Line section of the SPM image (2D).

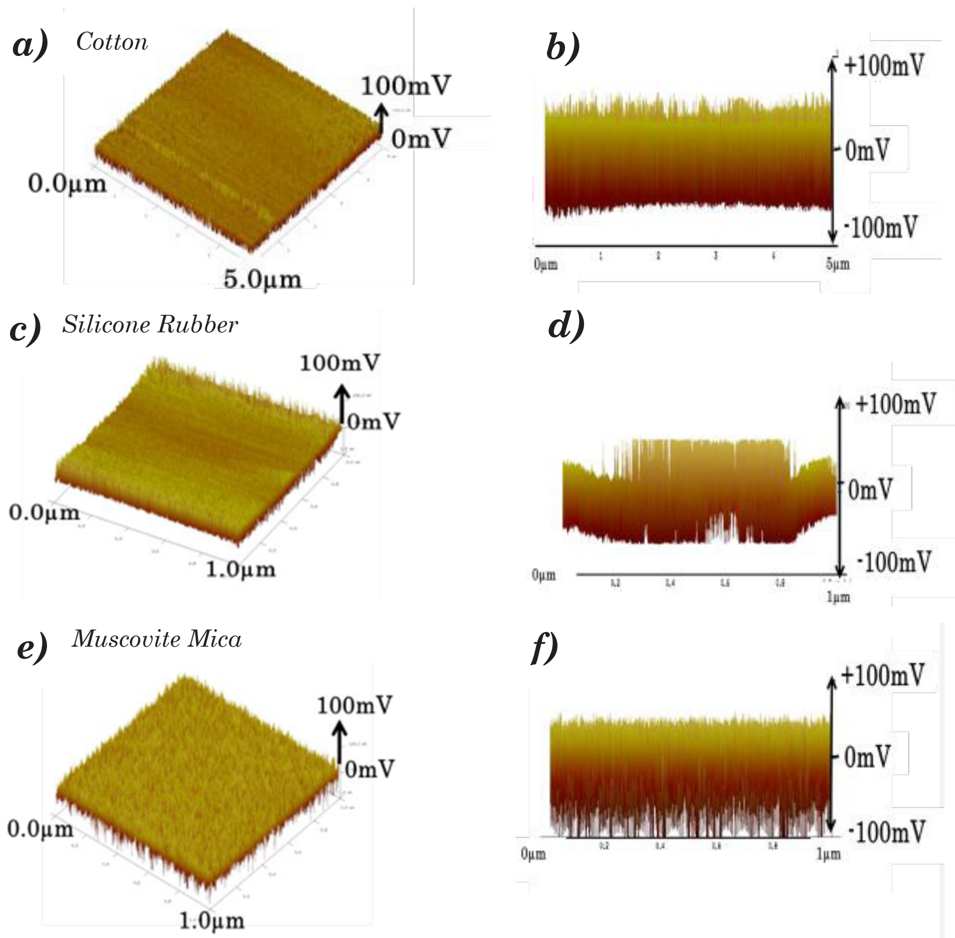

Figure 7. KFM image of Si (100) after CE using cotton (5 µm × 5 µm), mica, and silicone rubber.

Figures 7E and 7F show the KFM image of the Si sample after being applied CE using mica sheet. Mica has higher positive (+) charge affinity compared to cotton; Si on the other hand is negative (–), so the resulting KFM image has shown negative potential peaks as shown in Figures 7E and 7F.

Decay Time

It was reported for polymers that there is a minimal average reduction after 2.2 hours for insulator-like polymers (Baytekin et. al., 2011). In order to understand the behavior of the surface charge in Si after extended periods of time, surface charge retention was taken after grounding the sample. The sample was placed on a stainless steel disk fixture 30 mm in diameter and 3 mm in thickness and was attached to conductive carbon tape with surface resistance of <10^5 Ω. The setup allows the sample to be electrically grounded from the fixture to AFM base plate. This setup allows the sample to be continuously discharged during the acquisition of the image in the SPM tapping mode. Contact electrification was performed again using the same method as previously described. SPM scanning duration took about 1,080 seconds (~0.3 hour) from contact electrification, which includes tip engagement; loading on the sample ~100 *seconds*; and actual scanning, which takes another ~980 *seconds*. Figure 8 (A to E) shows the sequence of surface charge images by SPM. In Figure 8A, the initial image is recorded after 50 seconds. Minimal change had been observed on the average surface potential from A to B; in C, the image shows some spikes appearing along the edges of the surfaces, but subsequently, these spikes are reduced as shown in D (after 550 seconds). Both positive and negative surface charge distributions on Si (100) wafer have dissipated in the order of ±2.5 *mV* after 4800 seconds of noncontact electrification.

Figure 8E shows the potential profile with very small texture, suggesting the surface potential has decayed to 0. These observations are similar to the previous work

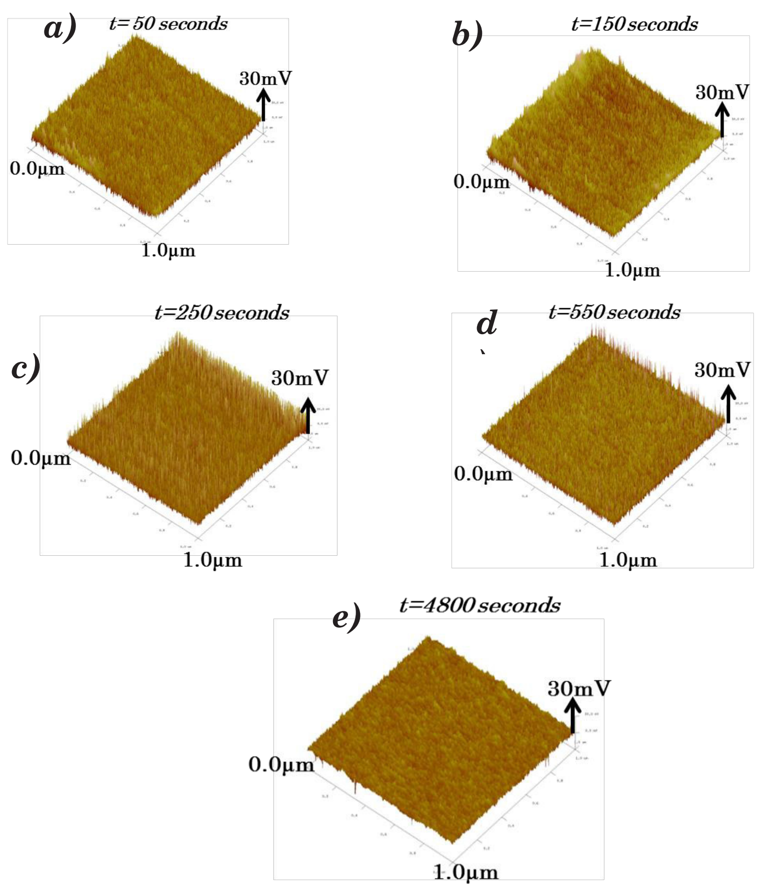

Figure 8. Surface potential profile and decay time.

on CE showing that Si (111) is stable after 800 seconds (Shiota, n.d.), which indicated a long relaxation time.

The average surface height deviation was used to measure changes in surface potential value of Figures 8A to 8E. These values are referred to as average roughness (*Ra*) using NanoScope software ver. 11 of the Bruker ICON AFM wherein the image selected through a cursor box calculates this value in millivolts.

Figure 9 (A to E) shows the temporal surface potential (in millivolts) of the Si wafer even after a period of 4800 seconds. The surface potentials are derived from the inset SPM images that were averaged from the entire surface area with height deviations.

The dynamics of the surface charge on the Si (100) wafer brought about by the triboelectrification can be modeled like a D.C. electric circuit where the diode and a capacitor are connected in series as shown in Figure 10. It can deduce that the surface charge generated from the triboelectrification behaves like a capacitor-like element while the Si wafer–carbon conductive junction behaves like a diode.

Thus, the equivalent D.C. electric circuit can be treated like a clamped capacitor circuit where the surface charge is being discharged by the *n*-type Si/carbon conductive tape Schottky diode-like junction with a constant positive voltage in equation (2.0), which is the breakdown voltage of the Si wafer and carbon conductive tape junction. Thus, the decay time constant of the uniformly surface charge distribution in the capacitor like on the Si wafer can be described in terms of the potential difference between the cantilever and the grounded steel disk as Panofsky and Phillips (1978, p .123) show in Figure 10.

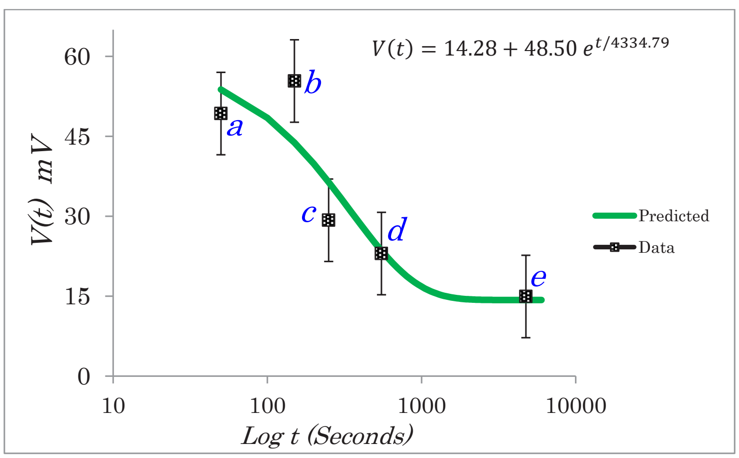

Figure 9. Plot of Si decay time.

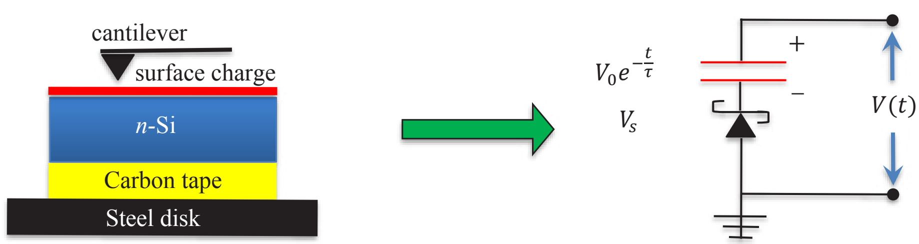

Figure 10. Equivalent D.C. circuit model.

$$V(t) = V_0 e^{-\frac{t}{\tau}} + V_s \qquad (5.0)$$

The electric potential measured by the surface potential mode of AFM is the total surface potential from the charging capacitor-like element with an initial surface potential of from triboelectrification and a constant positive potential due to the breakdown voltage of the n-type Si/carbon conductive tape Schottky junction. In equation (2.0), is considered the decay time constant of the air between the Si wafer and the cantilever of the AFM system. For the condition set in the experiment, decay time constant can be estimated as

$$\tau = \left(\varepsilon_{eff}\rho_{eff}\right) \qquad (6.0)$$

where is the effective relative permittivity of both air and silicon in Farad per meter and is the effective resistivity of both air and silicon in Ohm-meter. The relative electric permittivity of air at STP is = 8.9 x 10^{-12} F/m, and the relative permittivity of silicon is F/m, while the resistivity of air is = 1.3 x 10^{16} ~3.3 × 10^{17} Ω-m and the resistivity of silicon is 0.2 Ω-m («Properties of Silicon—El-Cat.com,» and Virginia Semiconductor Inc., n.d). For the composite material of air and silicon in the capacitor-like element, with common surface area A, the decay time constant can be calculated in terms of the permittivities and resistivities of both air and silicon respectively, that can be derived as

$$\tau = \varepsilon_{eff}\rho_{eff} = \frac{\varepsilon_{air}\varepsilon_{Si}(\rho_{air}d_{air}+\rho_{Si}d_{Si})}{\varepsilon_{Si}d_{air}+\varepsilon_{air}d_{Si}} \qquad (7.0)$$

In understanding how the capacitor and diode models are separated, the depth of the depletion region between n-type Si and carbon conductive tape (a Schottky diode-like element) provides the demarcation line between the capacitor and the diode models where the charge thickness d_{Si} of Si on the air-Si interface layer for the capacitor model is shown in Figure 11.

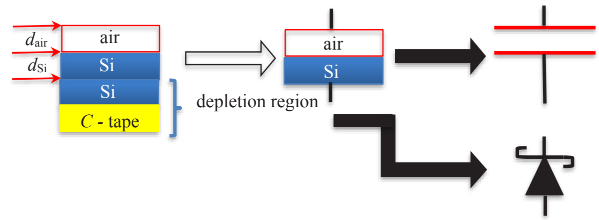

Figure 11. Depletion region.

Substituting the electric permittivities and resisitivities of both air and silicon materials, the charge thickness on air taken from SPM image (), the decay time constant from the fitted exponential green line from Figure 6, which is 4334.79 seconds, into equation (4) with a potential barrier of 15.6 mV for the n-type Si/carbon conductive tape Schottky diode-like junction and a surface potential of 48.5 mV, we can predict the depletion thickness of Si involved in discharging the surface charge as shown in Table 1

Table 1. List of Possible Depletion Thickness *d*Si (nm) of Si Involved in Discharging the Surface Charge Given Two Possible Input Parameters of *ρ*air and *d*air

Air Resistivity, ρair (Ω-m)	Air Thickness, dair (nm)	Depletion Thickness, dsi (nm)
1.3 × 1016	8	27
	16	5
3.3 × 1017	8	70
	16	14

with two different input parameters: the resistivity of air and the air gap thickness d_{air} taken from SPM measurements. It can be shown in Table 1 that the thickness of the Si wafer should be more than 70 nm to provide enough space for discharging the capacitor in the proposed model.

CONCLUSION

The surface charge on the Si (100) wafer was demonstrated using the tapping mode of KFM. KFM surface images of the Si (100) wafer after CE can have either more positive or negative peaks depending on the charge affinity of the material in contact. Also, it was determined that surface charge did not diminish up to 50% of its original surface charge even after 550 seconds. Surface potential distribution on the Si (100) wafer has relatively small potential change in the order of ±2.5 mV even after 4800 seconds of noncontact electrification. A direct current (D.C.) *electric circuit model*, which consists of a clamped capacitor in series with a Schottky diode, explains how the surface potential of the Si wafer is slowly diminished with a time constant of 4334.79 seconds and a breakdown voltage of 15.6 mV at the depletion region of Si/carbon tape interface.

ACKNOWLEDGEMENTS

The authors would like to give their sincerest appreciation to Misses Shirley Galicia and Allana Lopez for their assistance during AFM/ SPM setup. Also, the corresponding author would like to thank Messrs. Hidehiro Sakurai and Arun Khanna, for allowing the corresponding author some AFM time at TPC Reliability Engineering Laboratory.

REFERENCES

3" Cotton Applicator | Clean Cross. (n.d.). Retrieved from http://www.cleancross.net/english/products/threeinch_standard.html

AFM Probes | AFM Cantilever | AFM Tips—Bruker AFM Probes. (n.d.). Retrieved from http://www.brukerafmprobes.com/

Bailey, A. G. (2001). The charging of insulator surfaces. *Journal of Electrostatics*, *51–52*, 82–90.

Baril, L., Nichols, M., & Wallash, A. (2002). Degradation of GMR and TMR recording heads using very short duration ESD transients. *IEEE International Digest of Technical Papers on Magnetics Conference 38(5),2283-2285*.

Baytekin, B., Baytekin, H. T., & Grzybowski, B. A. (2012). What really drives chemical reactions on contact charged surfaces? *Journal of the American Chemical Society*, *134*(17), 7223–7226.

Baytekin, H. T., Patashinski, A. Z., Branicki, M., Baytekin, B., Soh, S., & Grzybowski, B. A. (2011). The mosaic of surface charge in contact electrification. *Science*, *333*(6040), 308–312.

Basic theory atomic force microscopy (AFM) [pdf]. (n.d.). Retrieved from http://asdlib.org/onlineArticles/ecourseware/Bullen/SPMModule_BasicTheoryAFM.pdf.

Brunkov, P. N., Goncharov, V. V., Rudinsky, M. E., Gutkin, A. A., Gordeev, N. Y., Lantratov, V. M.,… Konnikov, S. G. (2013). Local triboelectrification of an n-GaAs surface using the tip of an atomic-force microscope. *Semiconductors, 47*(9), 1170–1173.

Cai, W., & Yao, N. (2016). Dynamic nano-triboelectrification using torsional resonance mode atomic force microscopy. *Scientific Reports, 6*(1).

Diaz, A., & Felix-Navarro, R. (2004). A semi-quantitative tribo-electric series for polymeric materials: The influence of chemical structure and properties. *Journal of Electrostatics*, *62*(4), 277–290.

El-Mouloud Zelmat, M., Rizouga, M., Tilmatine, A., Medles, K., Miloudi, M., & Dascalescu, L. (2013). Experimental comparative study of different tribocharging devices for triboelectric separation of insulating particles. *IEEE Transactions on Industry Applications*, *49*(3), 1113–1118.

Gady, B., Reifenberger, R., & Rimai, D. S. (1998). Contact electrification studies using atomic force microscope techniques. *Journal of Applied Physics, 84*(1), 319–322.

KAB Electro Acoustics. (n.d.). Retrieved from http://www.kabusa.com

Hogue, M. (2004). Insulator/insulator contact charging and its relationship to atmospheric pressure . *Journal of Electrostatics*, *61*(3–4), 259–268.

Lacks, D. J., & Mohan Sankaran, R. (2011). Contact electrification of insulating materials. *Journal of Physics D: Applied Physics, 44*(45), 453001.

Mazur, T., & Grzybowski, B. A. (2017). Theoretical basis for the stabilization of charges by radicals on electrified polymers. *Chemical Science, 8*(3), 2025–2032.

Melitz, W., Shen, J., Kummel, A. C., & Lee, S. (2011). Kelvin probe force microscopy and its application. *Surface Science Reports, 66*(1), 1–27.

Muscovite Mica Substrates: SPI Supplies. (n.d.). Retrieved from http://www.2spi.com/category/mica-substrates/substrates/

Németh, E., Albrecht, V., Schubert, G., & Simon, F. (2003). Polymer tribo-electric charging: dependence on thermodynamic surface properties and relative humidity. *Journal of Electrostatics*, *58*(1–2), 3–16.

Panofsky, W. K., & Phillips, M. (1978). *Classical electricity and magnetism*. Mineola, NY: Dover Publications.

Part 5: Device Sensitivity and Testing » EOS/ESD Association, Inc. (n.d.). Retrieved from https://www.esda.org/about-esd/esd-fundamentals/part-5-device-sensitivity-and-testing/

Properties of Silicon—El-Cat.com. (n.d.). Retrieved from http://www.el-cat.com/silicon-properties.htm

Sakaguchi, M., Makino, M., Ohura, T., & Iwata, T. (2014). Contact electrification of polymers due to electron transfer among mechano anions, mechano cations and mechano radicals. *Journal of Electrostatics, 72*(5), 412–416.

Shiota. Retrieved from www.oetg.at/fileadmin/Dokumente/oetg/Proceedings/.../M-11-10-658-SHIOTA.pdf

Tipikin. (2002) Article retrieved from www.tipikindmitriy.hostoi.com/web_documents/part1.pdf

Virginia Semiconductor, Inc. (n.d.). Retrieved from http://www.virginiasemi.com

Williams, M. W. (2012). Triboelectric charging of insulating polymers–some new perspectives. *AIP Advances*, *2*(1), 010701.

Zhou, Y. S., Li, S., Niu, S., & Wang, Z. L. (2016). Effect of contact- and sliding-mode electrification on nanoscale charge transfer for energy harvesting. *Nano Research, 9*(12), 3705–3713.

Zhou, Y. S., Liu, Y., Zhu, G., Lin, Z., Pan, C., Jing, Q., & Wang, Z. L. (2013). In situ quantitative study of nanoscale triboelectrification and patterning. *Nano Letters*, *13*(6), 2771–2776.